Geosci. Model Dev. Discuss., 3, 1317–1357, 2010
www.geosci-model-dev-discuss.net/3/1317/2010/
doi:10.5194/gmdd-3-1317-2010

Geoscientific Model Development Discussions

Development and validation of a size-resolved particle dry deposition scheme for applications in aerosol transport models

A. Petroff[1,*] **and L. Zhang**[1]

[1]Air Quality Research Division, Science and Technology Branch, Environment Canada, 4905 Dufferin Street, Toronto, Ontario M3H 5T4, Canada
[*]now at: The University of Toronto, Department of Chemistry, 80 St George Street, Toronto, Ontario M5S 3H6, Canada

Received: 1 August 2010 – Accepted: 2 August 2010 – Published: 19 August 2010

Correspondence to: A. Petroff (alexandre.petroff@utoronto.ca),
L. Zhang (leiming.zhang@ec.gc.ca)

Published by Copernicus Publications on behalf of the European Geosciences Union.

Abstract

A size-resolved particle dry deposition scheme is developed, which has been designed for inclusion in large-scale air quality and climate models, where the size distribution and fate of the atmospheric aerosol is of concern. The "resistance" structure is similar to what is proposed by Zhang et al. (2001, 2003), while a new "surface" deposition velocity (or surface resistance) is derived by simplification of a one-dimensional aerosol transport model (Petroff et al., 2008b, 2009). Collection efficiencies are given for the 26 Land Use Categories that decribe the earth surface. Validation of this model with existing measurements is performed on desert, grass, coniferous forest and liquid water surfaces. A comparison of this model with measurements on snow and ice is also given. Even though a qualitative agreement is reached, further size-segegated measurements are needed in order to confirm the model accuracy on this surface. The present analytical model provides more accurate predictions of the aerosol deposition on these surfaces than previous models.

1 Introduction

Atmospheric aerosols are responsible for increased human mortality and morbidity (Lippmann et al., 2003; Kappos et al., 2004; Englert, 2004), ecosystem acidification and eutrophication (Fowler et al., 2009, and references therein), crop contamination by genetically modified spores (e.g. Jarosz et al., 2004), and for the forcing of the radiative balance of the atmosphere (IPCC, 2007). Their fate in the atmosphere and on earth can be predicted by chemical transport models of pollution or climate models (Gong et al., 2003; Bessagnet et al., 2004; Textor et al., 2006), but it requires an adequate, though simple enough, description of their dry deposition fluxes on the earth surface.

Many of the size-dependent dry deposition models apply only to one type of surface such as grass or vegetation canopies (e.g. Davidson et al., 1982; Slinn, 1982) while other models were developed for any type of surface (Sehmel and Hodgson, 1978; Giorgi, 1986; Zhang et al., 2001; Nho-Kim et al., 2004). Comparisons of several

GMDD

3, 1317–1357, 2010

models (Ruijgrok et al., 1995; Petroff et al., 2008a) revealed that they differ from each other greatly and the largest uncertainty is for the 0.1–1.0 micron particle size range. In this size range, the predicted deposition velocity V_d, defined as the ratio of the particle flux to the concentration at a reference height, can vary over two orders of magnitude on vegetation. In fact, most models developed before the 1990s are based on wind-tunnel measurements on low roughness canopies (in particular Chamberlain, 1967) and suggest that particles in the range of 0.1–1.0 micron diameter should have deposition velocity (V_d) values around 0.01 cm s^{-1}, which are much smaller values than more recent measurements obtained on rougher canopies such as forests (e.g. Buzorius et al., 2000; Pryor et al., 2007; Grönholm et al., 2009).

Modelling the deposition of aerosol requires to describe the vertical transport of particles by the turbulent flow from the overlaying atmosphere into the canopy, usually through a aerodynamic resistance, and the collection of the particles on the vegetation obstacles (leaves, twigs, trunks, flowers, and fruits). Particle collection on obstacles is driven by physical processes of Brownian diffusion, interception, inertial and turbulent impaction, gravitational settling and on water surfaces phoretic processes. These processes are accounted for in the models through efficiencies, that depend on the properties of the vegetation obstacles, the turbulent flow and the depositing aerosol particles. More details on the existing models are given in (Petroff et al., 2008a; Pryor et al., 2008).

Zhang et al. (2001) developed a size-resolved deposition model based on earlier models (Slinn, 1982; Giorgi, 1986) so the model produces higher V_d values for submicron particles than most earlier models (0.1–1 cm s^{-1} over vegetated surfaces). The model was constructed so as to produce higher V_d values over rougher and taller surfaces than over smoother surfaces, and also to produce higher V_d (especially for large particles) over needleleaf trees than over broadleaf trees. This model has been adopted by a large number of large-scale models around the world (Andersson et al., 2007; Ghan and Easter, 2006; Gong et al., 2006; Heald et al., 2006; Wang et al., 2006; Zakey et al., 2006).

GMDD
3, 1317–1357, 2010

Although the model of Zhang et al. (2001) seems to be able to produce more reasonable V_d values for submicron particles compared to many other existing models, the minimum V_d produced by this models is shifted to larger particle sizes (e.g., 1–2 µm) over several land use categories. The particular particle size for which the minimum V_d value is predicted to occur is decided by the relative magnitude of the collection efficiencies (Zhang and Vet, 2006). Since the collection efficiencies by Brownian diffusion, impaction and interception are expected to be different over different canopies, the minimum V_d should appear at different particle sizes over different canopies. Available measurements show that the minimum V_d should be located at particle sizes around 0.1–0.3 µm over some canopies, while some reviews mention the possibility for this minimum to be close to 1 µm over other canopies (Zhang and Vet, 2006; Pryor et al., 2008). The minimum V_d in many earlier models (Slinn, 1982; Davidson et al., 1982; Wiman and Agren, 1985) appears in the accumulation mode (0.08–1 µm).

A new and more sophisticated approach has been developed to model the transport and deposition of aerosol within vegetation composed either of cylindrical obstacles like needles (Petroff et al., 2008b) or of planes obstacles like broadleaves (Petroff et al., 2009). This one-dimensional model, hereafter referred to as "1-D-Model", is able to predict the proper particle size for minimum V_d while giving reasonable V_d values over grass and forest. However, this model only applies to vegetation canopies and is numerically too complex to be implemented in large-scale models.

The present paper deals with the description of an analytical and size-segregated aerosol dry deposition model, which resistive structure is the same as in the models of Zhang et al. (2001, 2003), while the improved parameterizations of the surface resistance and the different collection efficiencies are based on previous work (Petroff et al., 2008b, 2009). This model is initially designed for vegetative canopies, but its application is extended to other land-use categories, such as water surface, deserts and cities.

GMDD
3, 1317–1357, 2010

The theory on which the model is based is presented in the Sect. 2, regarding the aerodynamics and the aerosol transport. Then, in the Sect. 3, the model is implemented on different types of surface and compared with existing measurements.

2 Theoretical considerations

2.1 Aerodynamic model

Above the canopy, the inertial sub-layer is assumed to take place right on top of the canopy and can be described by the similarity theory of Monin and Obhukov (1954), even though this assumption can be questioned in the vicinity of rough canopies. There, the eddy diffusivities for heat and humidity indeed increase significantly compared to the theory in near-neutral to stable atmosphere (Fazu and Schwerdtfeger, 1989; Cellier and Brunet, 1992). The mean flow velocity U is classically estimated with the logarithmic law corrected for the stability:

$$U(z) = \frac{u_*}{\kappa}\left[\ln\left(\frac{z-d}{z_0}\right) - \Psi_m\left(\frac{z-d}{L_O}\right) + \Psi_m\left(\frac{z_0}{L_O}\right)\right], \quad (1)$$

where κ is the von Karman constant, hereafter taken equal to 0.4, z_0 and d are the roughness length and the displacement height of the canopy, u_* is the friction velocity above the canopy, L_O is the Obhukov length and Ψ_m the integrated form of the stability function for momentum. In this study, we are using the profiles of Paulson (1970); Dyer (1974) to describe the stability functions for momentum, heat, as well as their integrated form. Though classical, these formumations are recalled here in order to avoid confusion and inconsistency with the value of κ. The stability function is given by:

$$\Psi_m(x) = \begin{cases} 2\ln\left[\frac{1+(1-16x)^{\frac{1}{4}}}{2}\right] + \ln\left[\frac{1+(1-16x)^{\frac{1}{2}}}{2}\right] - 2\arctan\left[(1-16x)^{\frac{1}{4}}\right] + \pi/2 & \text{when } x \in [-2;0] \\ -5x \text{ when } x \in [0;1] \end{cases} \quad (2)$$

GMDD
3, 1317–1357, 2010

The aerosol eddy diffusivity is approached by the eddy diffusivity for heat:

$$K_p = l_{mp} u_* \quad \text{with} \quad l_{mp} = \frac{\kappa (z-d)}{\phi_h\left(\frac{z-d}{L_0}\right)}, \tag{3}$$

where l_{mp} is the mixing length for particles and ϕ is the stability function for heat. Its expression is $\phi_h(x) = (1-16x)^{-1/2}$ when $x \in [-2;0]$ and $\phi_h(x) = 1+5x$ when $x \in [0;1]$. The turbulent Schmidt number is thus taken in Eq. (3) equal to the turbulent Prandtl number. The aerodynamic resistance to the transport of particles between two heights z_1 and z_2 above the canopy, is written as:

$$R_a(z_1, z_2) = \frac{1}{\kappa u_*}\left[\ln\left(\frac{z_2-d}{z_1-d}\right) - \Psi_h\left(\frac{z_2-d}{L_O}\right) + \Psi_h\left(\frac{z_1-d}{L_O}\right)\right], \tag{4}$$

where Ψ_h is the integrated form of the stability function for heat. Its expression is $\Psi_h(x) = 2\ln\left[0.5(1+(1-16x)^{1/2})\right]$ when $x \in [-2;0]$ and $\Psi_h(x) = -5x$ when $x \in [0;1]$. For non-vegetated surfaces, whose roughnesses are not explicitly resolved, the aerodynamic resistance is written as:

$$R_a(z_0+d, z_R) = \frac{1}{\kappa u_*}\left[\ln\left(\frac{z_R-d}{z_0}\right) - \Psi_h\left(\frac{z_R-d}{L_O}\right) + \Psi_h\left(\frac{z_0}{L_O}\right)\right]. \tag{5}$$

Inside the canopy, we use a model based on a diffusive closure of the momentum flux and described by Inoue (1963). It is based on the assumption of constant drag coefficient, mixing length and leaf area density. This model is open to criticism because it assumes a local equilibrium between turbulence production and dissipation within the canopy (Kaimal and Finnigan, 1994). In practice though, such an equilibrium is not reached within the canopy because of the eddy transport term (see for example Brunet et al., 1994). Moreover, this closure is invalidated by experimental results, which show the existence of secondary maxima of the mean velocity occurring under the foliage crown and corresponding to negative values of the eddy diffusivity (Denmead

GMDD
3, 1317–1357, 2010

and Bradley, 1985). In the present study, this rudimentary model is used despite its limitations, because it leads to satisfactory predictions of the aerodynamic properties in the upper part of the canopy. This portion of canopy is of particular interest for aerosol deposition as it corresponds to strong mean flow velocity and local friction velocity, and subsequently, to large deposition fluxes. Using this model to describe the flow and the aerosol transport close to the ground might be more uncertain (see Grönholm et al., 2009, for particle flux measurements below the base of the canopy). This model predicts an exponential decrease of the mean wind velocity $U = \langle u \rangle$, particle eddy diffusivity K_p and local friction velocity u_f ($u_f^2 = -\langle u'' w'' \rangle$). The notation $\langle\ \rangle$ and $''$ refer respectively to the average over time and space and its fluctuations (see Petroff et al., 2008b for details). As an exemple, the mean wind velocity is written as:

$$U(z) = U_h \exp\left[\alpha\left(z/h - 1\right)\right], \tag{6}$$

where U_h is the horizontal mean flow velocity at the top of the canopy, measured on-site or estimated by Eq. (1), and α, the aerodynamic extinction coefficient, is identical for the three properties.

The impact of the atmospheric stability on the aerodynamics within the canopy is not fully understood and an adequate aerodynamic model within the vegetation roughnesses has still to be formulated (see Leclerc et al., 1990; Kaimal and Finnigan, 1994; Lee and Mahrt, 2005, for a study of stability influence on turbulence properties). The recent model of Harman and Finnigan (2007) should be mentioned as an alternative to describe the flow close to and within the roughnesses. Its main advantage is that it explicitly accounts for the extension of the roughness sub-layer above the canopy. But it cannot be used for now in an operational perspective because it strongly depends on the ratio u_*/U_h, which is highly variable with atmospheric stability.

In the present study, the influence of the stability is taken into account through the modification of aerodynamic properties above the canopy. As a consequence, the extinction coefficient depends on the stability through the mixing length (expressed on

GMDD
3, 1317–1357, 2010

the top of the canopy). It can be written as:

$$\alpha = \left(\frac{k_x \mathrm{LAI}}{12\kappa^2 \left(1 - d/h\right)^2} \right)^{1/3} \phi_m^{2/3} \left(\frac{h-d}{L_O} \right) \quad (7)$$

where k_x is the inclination coefficient of the canopy elements (see 1-D-model for the values of this parameter for different inclination distribution), LAI is the two-sided leaf area index, and ϕ_m is the non-dimensional stability function for momentum, whose expression is $\phi_m(x) = (1 - 16x)^{-1/4}$ when $x \in [-2;0]$ and $\phi_m(x) = 1 + 5x$ when $x \in [0;1]$. One should notice that the drag coefficient c_d and the displacement height d are assumed not to depend on the stability.

2.2 Aerosol transport model

The following assumptions are formulated to describe the canopy-aerosol system. The quasi-stationary state of the flow and the aerosol is reached. Canopy and aerodynamic mean properties are horizontally homogeneous. The canopy is treated solely in terms of the foliage, because its cumulative surface is greater than the surface of other components of the vegetation (though particle deposition in foliage absence could be easily studied if the description of the twig system is added to the model). The aerosol is considered as an homogeneous phase, in which particle-particle interactions, such as agglomeration or fragmentation, are not taken into account.

The hygroscopicity of particles is accounted for in the similar manner to Zhang et al. (2001). Depending on the aerosol size and chemical composition, as well as the ambient conditions, a wet particle diameter is calculated. Different formulas exist for this purpose in the litterature (Fitzgerald, 1975; Gerber, 1985; Zhang et al., 2005).

Rebound and resuspension of particles are not included in the present model, as it would require an adequate and simple parameterization of these processes and informations that are not available in transport models, such as a description of leaf surface

GMDD
3, 1317–1357, 2010

(micro-roughnesses, stickyness, wetness), the relative angle between the particle trajectory and the surface and the wind statistics. Interested readers should refer to Paw U (1983); Paw U and Braaten (1992); Wu et al. (1992a,b); Gillette et al. (2004).

The effects of the gravity and other drift forces such as phoretic effects are taken into account in a similar way as Slinn (1982); Zhang et al. (2001). Following the principle of superposition, their influence is estimated separately through a drift velocity V_{drift}. The deposition resulting from the turbulent transfer and the collection on leaves is estimated in a separate way as well. Both contributions are added and the deposition velocity at the reference height z_{R} is expressed by:

$$V_{\text{d}}(z_{\text{R}}) = V_{\text{drift}} + \frac{1}{R_{\text{a}}(h, z_{\text{R}}) + \frac{1}{V_{\text{ds}}}}, \tag{8}$$

where V_{ds} is the "surface" deposition velocity calculated on top of the surface roughnesses (its inverse is sometimes referred to as the surface resistance). The principle of surperposition is here abused, as gravity (and other drift effects) intervenes in the transport and the deposition of particle on the vegetation obstacles. Some studies reported that such approach is acceptable for one single obstacle exposed to the deposition of super-micronic particles (Yoshioka et al., 1972, cited by Bache, 1979).

In case of vegetated surfaces, the aerosol transport is resolved analytically within the canopy (see Sect. 2.2.2). For non-vegetated surfaces such as water surfaces (liquid and solid) as well as deserts and cities, a simplier surface deposition velocity is given in Sect. 2.2.3.

An approximated relation exists between deposition velocities estimated at different heights z_1, z_2:

$$\frac{1}{V_{\text{d}}(z_2) - V_{\text{drift}}} = \frac{1}{V_{\text{d}}(z_1) - V_{\text{drift}}} + R_{\text{a}}(z_1, z_2). \tag{9}$$

This relation, consistent with (Eq. 8), is used in the present paper. Though one should mention that it is an approximation that can induces an error of 15% on the recalculated

GMDD
3, 1317–1357, 2010

deposition velocity. For information, the exact relation is:

$$\frac{V_{\text{drift}}}{V_{\text{d}}(z_2)} - 1 = \left(\frac{V_{\text{drift}}}{V_{\text{d}}(z_1)} - 1\right) e^{-V_{\text{drift}} R_{\text{a}}(z_1, z_2)}. \quad (10)$$

2.2.1 Form of the drift velocity

The drift velocity V_{drift} is equal to the sedimentation velocity W_{S} for all surfaces except water, ice and snow surfaces, on which phoretic effects are also included through V_{phor}. These effects are related to important differences of temperature (thermophoresis, see for example Batchelor and Shen, 1985), water vapor (diffusiophoresis per se and Stefan flow effect Waldman and Schmitt, 1966; Goldsmith and May, 1966) or electricity (Tammet et al., 2001) between the collecting surfaces and the air. These effects can potentially affect the movement of particles. Thermophoresis and diffusiophoresis are likely to have an effect on fine particle deposition on liquid water surfaces (LUC 1, 3 and 23, Table 2). Phoretic effects induce a flux of particles toward cold and evaporating surfaces while the Stefan flow effect induces a flux of particles toward condensating surfaces. The full description of the corresponding balance require among other things the intensity of these gradients in the immediate vicinity of the surface, which is out of reach in the scope of this simple model. Therefore, we prefer to assign a constant small value of $5\times10^{-5}\,\text{m}\,\text{s}^{-1}$ to V_{phor} to water, ice and snow surfaces. This value is adjusted on an extended set of measurements obtained over water (see Fig. 6).

The importance of electrophoresis remains uncertain. Tammet et al. (2001) have compared the importance of electrical forces with other mechanical forces for a coniferous forest. They conclude that in typical atmospheric conditions, it might have an impact on the deposition of 0.01–0.2 µm particles on the tip of the top needles of trees and under very low-wind conditions, while effects might be sheltered within the canopy. It is presently unclear how this process might affect the deposition on the canopy as a whole. Thus, we prefer not to account for it in the parameterization of the drift velocity.

GMDD
3, 1317–1357, 2010

In the present study, the later is expressed by:

$$V_{\text{drift}} = W_{\text{S}} + V_{\text{phor}}, \tag{11}$$

with $V_{\text{phor}} = 5 \times 10^{-5}\,\text{m s}^{-1}$ for LUC 1, 2, 3, 23, and $V_{\text{phor}} = 0$ elsewhere.

2.2.2 Derivation of the surface deposition velocity for vegetated surfaces

Let γ be the aerosol mass concentration density averaged on time and space. Within the canopy, its balance equation is written as:

$$\frac{\text{d}}{\text{d}z}\left[K_{\text{p}}\frac{\text{d}\langle\gamma\rangle}{\text{d}z}\right] = a\langle\gamma\rangle V_{\text{T}}, \tag{12}$$

where a is the two-sided leaf area density and V_{T} is the total collection velocity on vegetation. Based on previous work, V_{T} can be written as:

$$V_{\text{T}}(z) = E_{\text{T}}(z)u_{\text{f}}(z) \quad \text{with} \quad E_{\text{T}} = \frac{U_{\text{h}}}{u_*}(E_{\text{B}} + E_{\text{IN}} + E_{\text{IM}}) + E_{\text{IT}}, \tag{13}$$

Where E_{T} is the total collection efficiency, and E_{B}, E_{IN}, E_{IM} and E_{IT} are the collection efficiencies corresponding to Brownian diffusion, interception, inertial impaction and turbulent impaction. In theory, these efficiencies depend on the altitude (see 1-D-model), but in the present study, they are considered to have a constant value, estimated on top of the canopy (see Table 1). In order to minimize the errors induced by this simplification, the numerical coefficients appearing in the efficiency formulation are adjusted with help of the 1-D-model. This fitting procedure is detailed in Sect. 2.2.5.

Considering efficiencies constant throughout the canopy allows us to derive an analytical solution to the mass balance (Eq. 12). Introducing the non-dimensional height $z^+ = z/h$ and concentration $\gamma^+ = \gamma(z)/\gamma(h)$ and accounting for the exponential profile of K_{p} (similar to Eq. 6), the mass balance (Eq. 12) can be rewritten as:

$$\frac{\text{d}^2\gamma^+}{\text{d}z^{+2}} + \alpha\frac{\text{d}\gamma^+}{\text{d}z^+} - Q\gamma^+ = 0 \quad \text{with} \quad Q = \frac{h \cdot \text{LAI} \cdot V_{\text{T}}}{K_{\text{p}}}. \tag{14}$$

GMDD
3, 1317–1357, 2010

The non-dimensional number Q (as notated by Fernandez de la Mora and Friedlander, 1982) corresponds to the ratio of the turbulent transport time scale to the vegetation collection time scale. Typically, $Q \ll 1$ corresponds to a situation of very efficient turbulent mixing while the transfer of particle is limited by the collection efficiency on leaves. This means an homogeneous particle concentration throughout the canopy. Meanwhile, $Q \gg 1$ corresponds to a situation where particles are so efficiently collected by leaves that their transfer to the surfaces is limited by the turbulent transport. It means an inhomogeneous particle concentration within the canopy. It can be rewritten as:

$$Q = \mathrm{LAI} \cdot E_\mathrm{T} \cdot h / l_\mathrm{mp}(h). \tag{15}$$

A boundary condition is required on the lower part of the canopy to describe the particle transfer to the ground. There, the flux is related to the concentration near the surface $\gamma^+(0)$ by a ground deposition velocity V_g:

$$\frac{\mathrm{d}\gamma^+}{\mathrm{d}z^+}(0) = Q_\mathrm{g}\gamma^+(0) \quad \text{with} \quad Q_\mathrm{g} = \frac{hV_\mathrm{g}}{K_\mathrm{p0}}, \tag{16}$$

where Q_g is the analog of Q for the transfer to the ground, and K_p0 is the value of the particle eddy diffusivity at its vicinity. The ground deposition velocity is related to the ground deposition efficiency by $V_\mathrm{g} = E_\mathrm{g} u_\mathrm{f}(0)$. The formulation of E_g is based on the assumption of smooth ground and is given in Sect. 2.2.4. The non-dimensional number Q_g can be rewritten as:

$$Q_\mathrm{g} = E_\mathrm{g} \cdot h / l_\mathrm{mp}(h). \tag{17}$$

One should note the strong similarities between the non-dimensional numbers Q and Q_g, and that the amount of leaves available for deposition, i.e. LAI, is explicitly appearing in the formulation of Q (Eq. 15). Assuming that the collection efficiencies, and thus Q and Q_g, are constant allows us to derive an analytical solution for the particle concentration:

$$\gamma^+ = \mathrm{e}^{\alpha/2(1-z^+)} \left[\frac{\eta\cosh\left(\eta z^+\right) + \left(Q_\mathrm{g} + \alpha/2\right)\sinh\left(\eta z^+\right)}{\eta\cosh(\eta) + \left(Q_\mathrm{g} + \alpha/2\right)\sinh(\eta)} \right] \quad \text{with} \quad \eta = \sqrt{\alpha^2/4 + Q}. \tag{18}$$

GMDD
3, 1317–1357, 2010

The deposition velocity on top of the canopy, i.e. the surface deposition velocity, corresponds to the ratio of the depositing flux on the canopy to the concentration on top of the canopy. It can be expressed as:

$$V_{ds}/u_* = V_g/u_*\gamma_0^+ + \mathrm{LAI}\cdot E_T \int_0^1 \gamma^+ e^{\alpha(z^+-1)} dz^+. \quad (19)$$

After some algebra, its formulation becomes:

$$\frac{V_{ds}}{u_*} = E_g \frac{1+\left[\frac{Q}{Q_g}-\frac{\alpha}{2}\right]\frac{\tanh(\eta)}{\eta}}{1+\left[Q_g+\frac{\alpha}{2}\right]\frac{\tanh(\eta)}{\eta}} \quad (20)$$

The Eq. (20) expresses the dependency of the surface deposition velocity on characteristics of the vegetation, the aerodynamics and the aerosol. One can thus wonder what would be the limit of the expression when the vegetation vanishes, i.e. when LAI$\to 0$ while $d/h \to 0$ (as prescribed by Raupach, 1994; 1995). In this case, $\alpha \to 0$, $\eta \to 0$ and $\tanh(\eta)/\eta \to 1$. As a consequence, $V_{ds}/u_* \to E_g/(1+Q_g)$ and the deposition velocity above the canopy is such that:

$$1/(V_d - V_{drift}) \to 1/(E_g u_*) + h/(u_* l_{mp}(h)) + R_a(h, z_R). \quad (21)$$

The second term on the right-hand side corresponds to the integration of $1/K_p$ over $[0, h]$ when $\alpha = 0$, and is equal to $R_a(0, h)$ (or $R_a(z_0, h)$ if we account for the roughness of the ground). As a consequence, $1/(V_d - V_{drift}) \to 1/(u_* E_g) + R_a(z_0, z_R)$, which is conform to the expectation that the surface deposition velocity for bare ground is driven by the deposition efficiency on the ground and the aerodynamic resistance.

GMDD
3, 1317–1357, 2010

2.2.3 Surface deposition velocity for non-vegetated surfaces

By extension of the asymptotic limit of Eq. (20) without vegetation, the deposition velocity for non-vegetated surfaces (liquid or solid water surfaces and desert) is simply:

$$V_d(z_R) = V_{drift} + \frac{1}{R_a(z_0, z_R) + 1/(E_g u_*)} \quad (22)$$

where the expression of E_g is detailed hereafter.

2.2.4 Parameterization of the ground deposition

The aerosol deposition on the ground below the vegetation canopy takes into account the Brownian diffusion and the turbulent impaction. Their respective deposition efficiencies, respectively E_{gb} and E_{gt}, are based on theoretical and empirical results obtained for pipes turbulent flow (see for example Davies, 1966; Papavergos and Hedley, 1984). The Brownian diffusion efficiency is expressed as:

$$E_{gb} = \frac{Sc^{-2/3}}{14.5}\left[\frac{1}{6}\ln\frac{(1+F)^2}{1-F+F^2} + \frac{1}{\sqrt{3}}\arctan\frac{2F-1}{\sqrt{3}} + \frac{\pi}{6\sqrt{3}}\right]^{-1}, \quad (23)$$

where F is a function of the Schmidt number expressed as $F = Sc^{1/3}/2.9$. An approximation of (23) given by Wood (1981) has been used by Petroff et al. (2009), but in the present study, we prefer to use the original formulation rather than the simplification proposed by Wood. This is because the later leads to significant errors for nano-particles: at 20 °C, the relative error is about 60% for 1 nm particles while it falls to about 5% for 14 nm particles.

The turbulent impaction efficiency term is similar to the one used to model deposition on vegetation (see Table 1) but is expressed on the ground, i.e. for a local friction velocity of $u_f = u_* e^{-\alpha}$. The constant C_{IT} is taken as 0.14. The latter is slightly different than previous work (0.18) but ensures the continuity of E_{IT} when $\tau_p^+ = 20$. This change does not affect the results of the 1-D-model in a significant way.

GMDD
3, 1317–1357, 2010

2.2.5 Parameterization of the collection efficiencies on leaves

The efficiencies with which physical processes intervene in aerosol deposition depend on the shape, dimensions and orientation of the elemental obstacles (leaf or needle). In the operational perspective, where such morphological and statistical details are out of reach, these dependencies are simplified in the following ways. The characteristic length L of the canopy obstacles is taken as the diameter for needles and as the mean width for leaves. It follows a Dirac distribution, i.e. each obstacle has the same size. A uniform distribution is assumed for the azimut angle. The inclination distribution is chosen as vertical for short grass, as erectophile for long grass and all the crop species, while forests and shrubs are described by the plagiophile distribution. Boundary-layers around obstacles are assumed to be laminar. The corresponding formulations of the efficiencies are based on the 1-D-model. They are briefly restated in Table 1. Sc is the Schmidt number ($Sc{=}\nu_a/D_B$, D_B being the coefficient of Brownian diffusion and ν_a air kinematic viscosity), Re_h is the Reynolds number of the flow estimated on top of the canopy ($Re_h = U_h L/\nu_a$, St_h is the Stokes number on top of the canopy ($St_h = \tau_p U_h/L$, with τ_p the relaxation time of the particle), τ^+_{ph} is the non-dimensional relaxation time of the particle on top of the canopy ($\tau^+_{ph} = \tau_p u_*^2/\nu_a$).

In theory, the constants C_B, C_{IN}, C_{IM} and C_{IT} appearing in Table 1 account for the chosen distributions of characteristic length and orientation of the obstacles. But in the present model, the efficiencies are taken constant throughout the canopy and the different constants have to be adjusted for each vegetated surfaces.

To do so, in a first step, probable variation ranges are defined for the main parameters of the two models, namely the friction velocity (3 values), the obstacle dimension (2 values), the ratios z_0/h (0.05–0.1) and d/h (0.65–0.85), LAI (2 values), particle density (1000–3000 kg m^{-3}) and the ratio of the foliage base height to the canopy heights (2 values, only for forest and shrubs). The combinations of these parameters gives us between 96 and 192 configurations. In a second step, the present model and the 1-D-model are run side by side under each of these configurations for particle size

GMDD
3, 1317–1357, 2010

between 1 nm and 1 mm. The relative error between them, Err, is used to estimate their agreement: Err=(V_d(1Dmodel) – V_d(present))/V_d(1Dmodel) and the coefficients C_B, C_{IN}, C_{IM}, and C_{IT} are adjusted in order to minimize the relative error. Such a fitting exercise is required for two reasons. The first is that the derivation of the present model assumes constant particle deposition efficiencies. The second reason is that the present model treats the vegetation surface as vertically uniform. This assumption induces biases with the 1-D-model in canopies such as forest, of which vegetation is concentrated in the upper-part of the canopy where the wind is strong. An example of the result of this procedure is shown on the Fig. 1 for the long grass canopy (LUC 14). Ratios of the fitted coefficients to original coefficients are 1.5, 1.2, 0.3, and 0.4 respectively for Brownian diffusion, interception, inertial impaction and turbulent impaction.

One should notice a bias that remains after the fitting for particles of a few microns under low wind conditions. It is due to the gravity, that acts in the 1-D-model as a collection efficiency on the leaves that are not vertical. Meanwhile, in the present model, gravity is not explicitly treated as a deposition mechanism within the canopy. This bias disappears quickly when the friction velocity increases and that other processes like interception and inertial impaction become active.

The values of C_B, C_{IN}, C_{IM} and C_{IT} resulting from this fitting procedure are given in Table 2.

2.2.6 Other parameters of the Land Use Categories

The other parameters describing the LUC are the mean height of the canopy h, the roughness length z_0 and the displacement height d, the two-sided leaf area index LAI and the characteristic obstacle length L. They are given in Table 2. The values of the roughness length and the leaf area index are given by Zhang et al. (2003). The LAI reported in Table 2 is twice the value given by Zhang et al., because they work with one-sided LAI. More details about the seasonal variation of z_0 and LAI are given by Zhang et al., in particular their Fig. 2 and Eq. (11). The values of canopy height and displacement are calculated based on the roughness length (Raupach et al., 1991):

GMDD
3, 1317–1357, 2010

$z_0/h = 0.06$ and $d/h = 0.80$ for forests (LUC 4 to 9 and 25, 26), where the maximum value of z_0 is used in the case of deciduous forest, $z_0/h = 0.13$ and $d/h = 0.64$ for shrubs (LUC 10 to 12) where the maximum value of z_0 is used in the case of deciduous shrubs; and $z_0/h = 0.13$ and $d/h = 0.64$ in the case of crops, grass, tundra, swamp (LUC 13 to 20 and 22, 23), where the canopy height is allowed to increase with the roughness length. The characteristic lengths of leaves and needles are estimates for each type of vegetation. The urban environment (LUC 21) is treated like in the global environmental multiscale (GEM) model with the LAI of 2 and the assumption that the urban trees are a mixture of needle- and broadleaf trees. This description is open to criticism and should be improved in the future.

3 Results

Results of the present models are evaluated in the following manner. First, its results are compared with the results of the 1-D-model on two typical vegetated canopies, in order to ensure the quality of the fit. Secondly, its results are compared to measurements obtained for different earth surfaces, such as desert, short grass, coniferous forest and water, both in liquid and solid phases.

3.1 Evaluation of the fit on two vegetation covers

Two typical vegetation covers of short grass (LUC 13) and coniferous forest (LUC 4) are chosen to compare in Fig. 2 the present model and the 1-D-model. The relative error is used as an indicator of agreement. The aerosol density is taken as $\rho_p = 1500\,\mathrm{kg\,m^{-3}}$ and different wind conditions are explored.

The evolution of the relative error depends on the acting deposition processes and the fitting constants. For these vegetation covers, it stays confined between −30 and 25%. One should notice that it returns to 0 when the particle diameter increases and that the sedimentation dominates the deposition.

GMDD
3, 1317–1357, 2010

The difference of treatement of the gravity appears for the coniferous forest under very light wind conditions, see Fig. 2d. There, the visible under-estimation of the aggretated model for particle between 1 and 10 µm is related to the fact that the inclinated leaves (plagiophile distribution) collect particles by gravity in the 1-D-model. Meanwhile, the present model does not account for sedimentation as a collection mechanism on the vegetation per se, but rather considers it as a process of deposition on the overall surface. For stronger wind, this bias disappears quickly.

3.2 Deposition on bare soil

We rely on experimental measurements of deposition on a smooth horizontal surface (Sehmel, 1973) to assess the validity of the parameterization of the ground deposition and evaluate the model on bare soil/desert (Eq. 22). The Fig. 3 presents the evolution of the deposition velocity at z_R=1 cm with particle diameter for three different flow conditions.

The evolution of the deposition velocity with particle diameter is reproduced by the model with some visible bias for coarse particles. The under-estimation of the model is maximum for particles between 5 and 15 µm and corresponds to a factor 2 to 4. This bias is associated with turbulent impaction, which remains a challenging process to measure or model (i.e. Young and Leeming, 1997; Guha, 2008) and should be confirmed by other measurements.

One should also notice on Fig. 3 the impact of the surface stickiness on the deposition of the coarsest particles by strong wind (last point of the data set corresponding to d_p=30 µm). The rebound, not accounted for in the present model, induces a marked over-estimation of a factor 4.

3.3 Deposition on short grass

Experiments performed on short grass (Chamberlain, 1967; Clough, 1975; Garland, 1983) and moorland (Gallagher et al., 1988; Nemitz et al., 2002) are used to evaluate

GMDD
3, 1317–1357, 2010

the performance of the present model fed with the parameters of LUC 13 (Tables 1 and 2). The two possible shapes of obstacle (plane or cylindrical) are investigated. The present model, the 1-D-model and the model of Zhang et al. (2001) are run for a friction velocity of $u_* = 40\,\mathrm{cm\,s^{-1}}$, which corresponds to the average friction velocity reported in the measurements ($u_* \in [25;55\,\mathrm{cm\,s^{-1}}]$). The atmosphere is assumed to be in near-neutral condition. A common height of 3.8 m is used to recalculate the deposition velocity (Eq. 9). This step has an significant impact on the deposition velocity of the coarse mode particles. Results are presented on Fig. 4.

One should notice a large dispersion within the measurements, which is not solely related to experimental uncertainty. Differences in canopy morphology (LAI, obstacle shape and obstacle size, $z0/h$, d/h as well and wind conditions have been proven to have a strong impact on the deposition (Davidson et al., 1982; Petroff et al., 2009, in particular Fig. 14 of the later). The shape of the obstacle is showed here to have a significant impact on the deposition too. Let every other parameter be the same, the deposition on grass composed of plane obstacles is larger than on grass composed of cylindrical obstacles. The difference can reach a factor 3 for accumulation mode particles. The reason for such a difference is to find in the different aerodynamics around a plane obstacle and around a cylinder (within the boundary-layer and above). As a result, the deposition efficiencies associated with Brownian diffusion, interception and impaction are strongly depending on the obstacle shape.

This comparison with measurements indicates reasonnable behaviours of both the leaf and the needle versions of the present model for any particle size. The model of Zhang et al. (2001) agrees with data for particle larger than some tenths of microns, but over-estimates the deposition of the smaller ones.

3.4 Deposition on coniferous forests

A similar comparison exercise is performed on forests of different coniferous species: spruce (Beswick et al., 1991), pine (Lorenz and Murphy, 1989; Lamaud et al., 1994; Buzorius et al., 2000; Gaman et al., 2004; Grönholm et al., 2009) and fir (Gallagher et al.,

GMDD
3, 1317–1357, 2010

1997). In these experiments, the friction velocity varies between 35 and 60 cm s^{-1} and the atmosphere was in a near-neutral condition. Models were fed with parameters of LUC 4 with a friction velocity of u_*=47.5 cm s^{-1} and particle density of ρ_p=1500 kg m^{-3}. All deposition velocities are recalculated at z_R=38 m (see Fig. 5).

A favorable agreement is found between these measurements and the present model, though some differences arise for large particle size. The later are due to the parameters chosen for running the models, that are not adequate to describe a lower and "smoother" forest, on which water droplets (smaller aerosol density) are transported by a slower flow (u_*=35 cm s^{-1}). Running the present model with the correct parameters (in blue dots on the Fig. 5) allows a better agreement with the data of Beswick et al. (1991) to be reached.

The model of Zhang et al. (2001) agrees relatively well with the same data, despite some criticisms regarding the location of the minimum deposition velocity in the coarse mode (Zhang and Vet, 2006).

3.5 Deposition over liquid water surfaces

We want to estimate the ability of this simple model (Eq. 22) to reproduce measurements on liquid water surfaces. Different campaigns on wind-tunnel (Möller and Schumann, 1970; Sehmel and Sutter, 1974) and on lake (Zufall et al., 1998; Caffrey et al., 1998) are used for this purpose. The relationship between the wind and the modification of the surface morphology (waves) is accounted for according to Charnock (1955) and Smith (1988). Under neutral conditions, mean wind, friction velocity and roughness length are related by:

$$z_0 = 0.11 \nu_a / u_* + 0.011 u_*^2 / g \quad \text{and} \quad u_* = \kappa U(z_R) / \ln(z_R / z_0). \tag{24}$$

This equation is used to calculate by iteration the friction velocity and the roughness length from the wind velocity. On the Fig. 6, we present together the results of the present model and the model of Zhang et al. (2001). All deposition velocity are recalculated at z_R=5.2 m using the Eq. (9).

GMDD
3, 1317–1357, 2010

Three wind regimes are represented on Fig. 6 with different colors: blue for low wind (u_*=11 cm s^{-1}), red for intermediate wind (u_*=44 cm s^{-1}), and green for strong wind (u_*=117 cm s^{-1}).

For fine particles under the lowest wind regime, Brownian diffusion is quite inefficient to deposit particles, in which case phoretic effects are likely to dominate. Setting the value of the corresponding drift velocity to $V_{phor} = 5 \times 10^{-3}$ cm s^{-1} allows us to reproduce well these data. For stronger wind, the brownian diffusion becomes efficient as the particle size decreases, which the present model is able to reproduce with a slight under-estimation (see the data of Möller and Schumann, 1970). The model of Zhang et al. (2001) significantly over-estimates the measurements for this size range.

The deposition of coarser particles is driven by gravity when the wind is low and by gravity and turbulent impaction as the friction velocity increases. In most situations, a reasonable agreement is reached between the measurements and both the displayed models in low or strong winds. Some differences arise though for stronger winds and particles around 5–10 µm, for which an under-estimation of the present model is noticed (in most cases of a factor 2).

We emphasize that none of the measurements used in the present comparison reflects the situation of an ocean or a sea, where previous works indicate that under strong wind conditions there is an impact of spray formation on particles deposition (Williams, 1982; Hummelshöj et al., 1992; Pryor and Barthelmie, 2000). More experiments are needed to assess this effect, using preferably direct eddy-correlation measurements (see for example Norris et al., 2008).

3.6 Deposition over snow and ice surfaces

Snow and ice represent a significant portion of the earth surface and require to be adequately taken into account in transport models. Despite the importance of these surfaces, the direct measurements of aerosol fluxes providing some information about the aerosol size are sparse, relatively to liquid water surfaces. They are obtained on snow (Ibrahim et al., 1983; Duan et al., 1988) and ice (Nilsson and Rannik, 2001) and

GMDD
3, 1317–1357, 2010

the roughness length varies between 10^{-4} and 2×10^{-2} m (Nilsson et al. measured roughness length up to 0.3 m – 90 percentile – over rough ice floes). The predictions of the present model and of the model of Zhang et al. (2001) are compared with these experiments on Fig. 7.

One should note that the symbols and "error" bars on the Fig. 7 do not represent the same quantities. Ibrahim et al. (1983) give results in term of the mean and standard deviation over 4 measurements (see their Table 2). Results of Nilsson and Rannik (2001) are given as the median, minimum and maximum values over 2 unknown numbers of periods where size distributions are typical of ultra-fine or Aitken particles. The results of Duan et al. (1988) are given in the present paper as the median, 25 and 75 percentiles of 28 half-hour datapoints.

If both models agree with measurements in the coarse mode, they give different results for fine particles. When considering the mean or median of the measures, the present model seems to under-estimate results by a factor 3 to 6. Meanwhile, Zhang et al's model seems to over-estimate Aitken particle deposition by a factor of 10 and agrees with results for the accumulation mode. Of course, the significant measurement uncertainty limits our ability to conclude. Moreover, it is unclear to us why deposition over snow and ice would be larger than deposition on water (see Fig. 6). In an effort to interpret their results, Ibrahim et al. (1983) invoke strong humidity gradients close to the snow ground that would affect ammonium sulfate particles and allow them to grow by hygroscopicity. Experiments, over longer periods of time and with measures of the humidity gradient close to the ground, would be useful to firmly evaluate the validity of the present model on ice and snow surfaces.

4 Conclusions and perspectives

In the present paper, we proposed an analytical model to predict the deposition of aerosols of different size on the earth surface. It updates the model of Zhang et al. (2001) and accounts for the morphology of the surface cover, the aerodynamics and the

GMDD
3, 1317–1357, 2010

aerosol properties. In particular, surface parameters such as the leaf area index or the size of the leaves are explicitly described and allows the model to be more sensitive to surface change (see Fig. 2 or the influence of the obstacle shape on Fig. 4). This model has been compared with measurements and gives reasonnable results for desert (see Fig. 3), vegetation covers (short grass, see Fig. 4, and coniferous forest, see Fig. 5) and liquid water surface (see Fig. 6). As expected, the deposition rate is larger over coniferous forest than over grass (see Fig. 2). Based on the reviewed measurements, the minimum of deposition velocity is placed in the accumulation mode, which the present model is able to predict.

A way to account for the atmospheric stability within the canopy is proposed in the present paper but is not validated by measurements. This should be the focus of future work.

The rebound and the resuspension could be included in the future if one would be able to inform the characteristics of the deposition surface and the state of the aerosol and to derive simple enough formulations of these complex processes.

The present model has still to be compared with size-segregated measurements obtained in urban centers. Aerosol fate might be difficult to predict as there are strong evidences that the particle flux over urban centers is mostly directed upward and corresponds to traffic-related emission (Dorsey et al., 2002; Mårtensson et al., 2006; Schmidt and Klemm, 2008). Consequently, the modelling of the aerosol fluxes over cities requires the description of the balance between particle emission and deposition. This should be the focus of future research.

GMDD
3, 1317–1357, 2010

Appendix A

Notations

C_C	Cunningham correction factor $C_C = 1 + 2\lambda/d_p(1.257 + 0.400e^{-1.1d_p/(2\lambda)})$	[-]	d	displacement height	[m]
D_B	Brownian diffusivity $D_B = C_C k_B T/(3\pi\mu_a d_p)$	[$m^2\,s^{-1}$]	d_p	particle diameter	[m]
E_T, E_B, E_{IN}, E_{IM}	Deposition efficiencies on the foliage	[-]	g	gravity acceleration	[$m\,s^{-2}$]
E_g	Deposition efficiency to the ground	[-]	h	mean canopy height	[m]
K_p	Particle eddy diffusivity	[$m^2\,s^{-1}$]	h_c	mean height of the crown base	[m]
L	Obstacle characteristic dimension	[m]	k_B	Boltzman constant $k_B = 1.38\times10^{-23}$	[$J\,K^{-1}$]
L_O	Obhukov length	[m]	k_x	inclination coefficient of the canopy elements	[-]
LAI	Two-side leaf area index	[-]	l_{mp}	mixing length for particles	[m]
Q, Q_g	non-dimensional numbers	[-]	u_f	local friction velocity	[$m\,s^{-1}$]
R_a	Aerodynamic resistance	[$s\,m^{-1}$]	u_*	friction velocity	[$m\,s^{-1}$]
Re_h	Reynolds number on top of the canopy	[-]	z_0	roughness length	[m]
Sc	Schmidt number	[-]	κ	Von Kärman constant	[-]
St_h	Stokes number on top of the canopy	[-]	Ψ_m, Ψ_h	integrated forms of the stability function for momentum and heat	[-]
T	Temperature, taken as 293, if not otherwise stated	[K]	ϕ_h	stability function for heat	[-]
U	Horizontal mean flow velocity	[$m\,s^{-1}$]	α	aerodynamic extinction coefficient	[-]
V_d	Deposition velocity	[$m\,s^{-1}$]	γ	aerosol mass concentration density	[$kg\,m^{-4}$]
V_{drift}	Drift velocity	[$m\,s^{-1}$]	η	non-dimensional number	[-]
V_g	ground deposition velocity	[$m\,s^{-1}$]	μ_a	air dynamic viscosity $\mu_a = 1.89\times10^{-5}$	[$kg\,m^{-1}\,s^{-1}$]
V_{phor}	phoretic drift velocity	[$m\,s^{-1}$]	ν_a	air kinematic viscosity $\nu_a = 1.57\times10^{-5}$	[$m^2\,s^{-1}$]
V_T	total collection velocity on vegetation	[$m\,s^{-1}$]	τ_p^+	non dimensional particle relaxation time	[-]
W_S	sedimentation velocity $W_S = g\tau_p$	[$m\,s^{-1}$]	τ_p	particle relaxation time $\tau_p = C_C\rho_p d_p^2/(18\mu_a)$	[s]
a	Two-side leaf area density	[m^{-1}]	ρ_p	particle density	[$kg\,m^{-3}$]

GMDD
3, 1317–1357, 2010

References

Andersson, C., Langner, J., and Bergström, R.: Interannual variation and trends in air pollution over Europe due to climate variability during 1958–2001 simulated with a regional CTM coupled to the ERA40 reanalysis, Tellus B, 59, 77–98, 2007. 1319

Bache, D.: Particle transport within plant canopies. I. A framework for analysis, Atmos. Environ., 13, 1257–1262, 1979. 1325

Batchelor, G. and Shen, C.: Thermophoretic deposition in gas flow over cold surfaces, J. Colloid Interf. Sci., 107, 21–37, 1985. 1326

Bessagnet, B., Hodzic, A., Vautard, R., Beekmann, M., Cheinet, S., Honoré, C., Liousse, C., and Rouil, L.: Aerosol modelling with CHIMERE-preliminary evaluation at the continental scale, Atmos. Environ., 38, 2803–2817, 2004. 1318

Beswick, K., Hargreaves, K., Gallagher, M., Choularton, T., and Fowler, D.: Size-resolved measurements of cloud droplet deposition velocity to a canopy using an eddy correlation technique, Q. J. Roy. Meteor. Soc., 117, 623–645, 1991. 1335, 1336, 1355

Brunet, Y., Finnigan, J., and Raupach, M.: A wind Tunnel study of Air Flow in Waving Wheat: Single point velocity statistics, Bound.-Lay. Meteorol., 70, 95–132, 1994. 1322

Buzorius, G., Rannik, Ü., Mäkelä, J., Vesala, T., and Kulmala, M.: Vertical aerosol fluxes measured by eddy covariance methods and deposition of nucleation mode particles above a Scots pine forest in southern Finland, J. Geophys. Res., 105, 19905–19916, 2000. 1319, 1335, 1355

Caffrey, P., Ondov, J., Zufall, M., and Davidson, C.: Determination of size-dependent dry particle deposition velocities with multiple intrisic elemental tracers, Environ. Sci. Technol., 32, 1615–1622, 1998. 1336, 1356

Cellier, P. and Brunet, Y.: Flux-gradient relationships above tall plant canopies, Agr. Forest Meteorol., 58, 93–117, 1992. 1321

Chamberlain, A.: Transport of *Lycopodium* spores and other small particles to rough surfaces, P. R. Soc. London, 296, 45–70, 1967. 1319, 1334, 1354

Charnock, H.: Wind stress on a water surface, Q. J. Roy. Meteor. Soc., 81, 639–640, 1955. 1336

Clough, W.: The deposit of particles on moss and grass surfaces, Atmos. Environ., 9, 1113–1119, 1975. 1334, 1354

Davidson, C., Miller, J., and Pleskow, M.: The influence of surface structure on predicted par-

GMDD
3, 1317–1357, 2010

ticle dry deposition to natural grass canopies, Water Air Soil Poll., 18, 25–43, 1982. 1318, 1320, 1335
Davies, C.: Deposition from moving aerosols, in: Aerosol science, edited by: Davies, C. N., Academic Press, London, UK, 393–446, 1966. 1330
Denmead, O. and Bradley, E.: Flux-gradient relationships in a forest canopy, in: The Forest-Atmosphere Interaction, edited by: Hutchinson, B. and Hicks, B. B., D. Reidel Publishing Company, Dordrecht, 421–442, 1985. 1322
Dorsey, J., Nemitz, E., Gallagher, M.W. Fowler, D., Williams, P., Bower, K., and Beswick, K.: Direct measurements and parameterisation of aerosol flux, concentration and emission velocity above a city, Atmos. Environ., 36, 791–800, 2002. 1339
Duan, B., Fairall, C., and Thomson, D.: Eddy-correlation measurements of the dry deposition of particles in wintertime, J. Appl. Meteorol., 27, 642–652, 1988. 1337, 1338, 1357
Dyer, A.: A review of flux-profile relationships, Bound.-Lay. Meteorol., 7, 363–372, 1974. 1321
Englert, N.: Fine particles and human health – a review of epidemiological studies, Toxicol. Lett., 149, 235–242, 2004. 1318
Fazu, C. and Schwerdtfeger, P.: Flux-gradient relationships for momentum and heat over a rough natural surface, Q. J. Roy. Meteor. Soc., 115, 335–352, 1989. 1321
Fernandez de la Mora, F. and Friedlander, S.: Aerosol and gaz deposition of particles to fully rough surfaces, Int. J. Heat Mass Tran., 26, 1725–1735, 1982. 1328
Fitzgerald, J.: Approximation formulas for equilibrium size of an aerosol particle as a function of its dry size and composition and ambient relative humidity, J. Appl. Meteorol., 14, 1044–1049, 1975. 1324
Fowler, D., Pilegaard, K., Sutton, M. A., Ambus, P., Raivonen, M., Duyzer, J., Simpson, D., Fagerli, H., Fuzzi, S., Schjoerring, J. K., Granier, C., Neftel, A., Isaksen, I. S. A., Laj, P., Maione, M., Monks, P. S., Burkhardt, J., Daemmgen, U., Neirynck, J., Personne, E., Wichink-Kruit, R., Butterbach-Bahl, K., Flechard, C., Tuovinen, J. P., Coyle, M., Gerosa, G., Loubet, B., Altimir, N., Gruenhage, L., Ammann, C., Cieslik, S., Paoletti, E., Mikkelsen, T. N., Ro-Poulsen, H., Cellier, P., Cape, J. N., Horvath, L., Loreto, F., Niinemets, U., Palmer, P. I., Rinne, J., Misztal, P., Nemitz, E., Nilsson, D., Pryor, S., Gallagher, M. W., Vesala, T., Skiba, U., Brueggemann, N., Zechmeister-Boltenstern, S., Williams, J., O'Dowd, C., Facchini, M. C., de Leeuw, G., Flossman, A., Chaumerliac, N., and Erisman, J. W.: Atmospheric composition change: Ecosystems-Atmosphere interactions, Atmos. Environ., 43, 5193–5267, 2009. 1318
Gallagher, M., Beswick, K., Duyzer, J., Westrate, H., Choularton, T., and Hummelshöj, P.:

GMDD
3, 1317–1357, 2010

Measurements of aerosol fluxes to Speulder forest using a micrometeorological technique, Atmos. Environ., 31, 359–373, 1997. 1335, 1355
Gallagher, W., Choularton, T., Morse, A., and Fowler, D.: Measurements of the size dependence of cloud droplet deposition at a hill site, Q. J. Roy. Meteor. Soc., 114, 1291–1303, 1988. 1334, 1354
Gaman, A., Rannik, Ü., Aalto, P., Pohja, T., Siivola, E., Kulmala, M., and Vesala, T.: Relaxed eddy accumulation system for size resolved aerosol particle flux measurements, J. Atmos. Ocean. Tech., 21, 933–943, 2004. 1335, 1355
Garland, J.: Dry deposition of small particles to grass in field conditions, in: Precipitation scavenging, dry deposition and resuspension, edited by: Pruppacher, H., Semonin, R., and Slinn, W., Elsevier, Amsterdam, Nederlands, 2, 849–857, 1983. 1334, 1354
Gerber, H.: Relative-humidity parameterization of the Navy aerosol model (NAM), in: NRL Report 8956, National Research Laboratory, Washington DC, 1985. 1324
Ghan, S. J. and Easter, R. C.: Impact of cloud-borne aerosol representation on aerosol direct and indirect effects, Atmos. Chem. Phys., 6, 4163–4174, doi:10.5194/acp-6-4163-2006, 2006. 1319
Gillette, D., Lawson Jr., R., and Thompson, R.: A "test of concept" comparison of aerodynamic and mechanical resuspension mechanisms for particles deposited on field rye grass (Secale cercele) – Part 2. Threshold mechanical energies for resuspension particle fluxes, Atmos. Environ., 38, 4799–4803, 2004. 1325
Giorgi, F.: A particle dry deposition parameterisation scheme for use in tracer transport models, J. Geophys. Res., 91, 9794–9806, 1986. 1318, 1319
Goldsmith, P. and May, F.: Diffusiophoresis and thermophoresis in water vapour systems, in: Aerosol science, edited by: Davies, C. N., Academic Press, London, UK, 163–194, 1966. 1326
Gong, S., Barrie, L., Blanchet, J.-P., von Salzen, K., Lohmann, U., Lesins, G., Spacek, L., Zhang, L., Lin, H., Leaitch, R., Leighton, H., Chylek, P., and Huang, S.: Canadian aerosol module: a size-segretated simulation of atmospheric aerosol processes for climate and air quality models. 1. Model development, J. Geophys. Res., 107(D24), 4779, doi:10.1029/2001JD002004, 2003. 1318
Gong, W., Dastoor, A., Bouchet, V., Gong, S., Makar, P., Moran, M., Pabla, B., Ménard, S., Crevier, L.-P., Cousineau, S., and Venkatesh, S.: Cloud processing of gases and aerosols in a regional air quality model (AURAMS), Atmos. Res., 82, 248–275, 2006. 1319

GMDD
3, 1317–1357, 2010

Grönholm, T., Launiainen, S., Ahlm, L., Mårtensson, E., Kulmala, M., Vesala, T., and Nilsson, E.: Aerosol particle dry deposition to canopy and forest floor measured by two-layer eddy covariance system, J. Geophys. Res., 114, D04202, doi:10.1029/2008JD010663, 2009. 1319, 1323, 1335, 1355
Guha, A.: Transport and deposition of particles in turbulent and laminar flow, Annu. Rev. Fluid Mech., 40, 311–341, 2008. 1334
Harman, I. and Finnigan, J.: A simple unified theory for flow in the canopy and roughness sublayer, Bound.-Lay. Meteorol., 123, 339–363, 2007. 1323
Heald, C., Jacob, D., Park, R., Alexander, B., Fairlie, T. D., Yantosca, R., and Chu, D. A.: Transpacific transport of Asian anthropogenic aerosols and its impact on surface air quality in the United States, J. Geophys. Res., 111, D14310, doi:10.1029/2005JD006847, 2006. 1319
Hummelshöj, P., Jensen, N. O., and Larsen, S. E.: Particle dry deposition to a Sea Surface, in: Fifth International Conference on Precipitation Scavenging and Atmosphere-Surface Exchange Processes. AMS, Richland, Washington, USA, 1992. 1337
Ibrahim, M., Barrie, L., and Fanaki, F.: An experimental and theoretical investigation of the dry deposition of particles to snow, pine trees and artificial collectors, Atmos. Environ., 17, 781–788, 1983. 1337, 1338, 1357
Inoue, E.: On the turbulent structure of airflow within crop canopies, J. Meteorol. Soc. Jpn., 11, 18–22, 1963. 1322
IPCC: Climate Change 2007: The Physical Science Basis, in: Contribution of Working Group I to the Fourth Assessment Report of the Intergovernmental Panel on Climate Change, Cambridge University Press, Cambridge, UK and New York, NY, USA, 2007. 1318
Jarosz, N., Loubet, B., and Huber, L.: Modelling airborne concentration and deposition rate of maize pollen, Atmos. Environ., 38, 5555–5566, 2004. 1318
Kaimal, J. and Finnigan, J.: Flow over plant canopies, in: Atmospheric Boundary Layer Flows, Oxford University Press, New York, USA, 1994. 1322, 1323
Kappos, A., Bruckmann, P., Eikmann, T., Englert, N., Heinrich, U., Hoppe, P., Koch, E., Krause, G., Kreyling, W., Rauchfuss, K., Rombout, P., Schulz-Klemp, V., Thiel, W., and Wichmann, H.: Health effects of particles in ambient air, Int. J. Hyg. Envir. Heal., 207, 399–407, 2004. 1318
Lamaud, E., Brunet, Y., Labatut, A., Lopez, A., Fontan, J., and Druilhet, A.: The Landes Experiment: Biosphere-atmosphere exchanges of ozone and aerosol particles above a pine forest,

GMDD
3, 1317–1357, 2010

J. Geophys. Res., 99, 16511–16521, 1994. 1335, 1355
Leclerc, M., Shaw, R., Den Hartog, G., and Neumann, H.: The influence of atmospheric stability on the budgets of the Reynolds stress and turbulent kinetic energy within and above a deciduous forest, J. Appl. Meteorol., 29, 916–933, 1990. 1323
Lee, Y. and Mahrt, L.: Effect of stability on mixing in open canopies, Agr. Forest Meteorol., 135, 169–179, 2005. 1323
Lippmann, M., Frampton, M., Schwartz, J., Dockery, D., Schlesinger, R., Koutrakis, P., Froines, J., Nel, A., Finkelstein, J., Godleski, J., Kaufman, J., Koenig, J., Larson, T., Luchtel, D., Liu, L., Oberdorster, G., Peters, A., Sarnat, J., Sioutas, C., Suh, H., Sullivan, J., Utell, M., Wichmann, E., and Zelikoff, J.: The US Environmental Protection Agency particulate matter health effects research centers program: A midcourse report of status, progress, and plans, Environ. Health Persp., 111, 1074–1092, 2003. 1318
Lorenz, R. and Murphy, J.: Dry deposition of particles to a pine plantation, Bound.-Lay. Meteorol., 46, 355–366, 1989. 1335, 1355
Mårtensson, E., Nilsson, E., Buzorius, G., and Johansson, C.: Eddy covariance measurements and parameterisation of traffic related particle emissions in an urban environment, Atmos. Chem. Phys., 6, 769–785, doi:10.5194/acp-6-769-2006, 2006. 1339
Möller, U. and Schumann, G.: Mechanisms of transport from the atmosphere to the earth's surface, J. Geophys. Res., 75, 3014–3019, 1970. 1336, 1337, 1356
Monin, A. and Obhukov, A.: Basic laws of turbulent mixing in the ground layer of the atmosphere, Akademiia Nauk SSSR, Leningrad, Geofizicheskii Institut, Trudy, and translated by the AMS, 24, 163–187, 1954. 1321
Nemitz, E., Gallagher, M., Duyzer, J., and Fowler, D.: Micrometeorological measurements of particle deposition velocities to moorland vegetation, Q. J. Roy. Meteor. Soc., 128, 2281–2300, 2002. 1334, 1354
Nho-Kim, E.-Y., Michou, M., and Peuch, V.-H.: Parametrization of size-dependent particle dry deposition velocity for global modeling, Atmos. Environ., 38, 1933–1942, 2004. 1318
Nilsson, E. and Rannik, Ü.: Turbulent aerosol fluxes over the Arctic Ocean 1. Dry deposition over sea and pack ice, J. Geophys. Res.-Atmos., 106, 32125–32137, 2001. 1337, 1338, 1357
Norris, S. J., Brooks, I. M., de Leeuw, G., Smith, M. H., Moerman, M., and Lingard, J. J. N.: Eddy covariance measurements of sea spray particles over the Atlantic Ocean, Atmos. Chem. Phys., 8, 555–563, doi:10.5194/acp-8-555-2008, 2008. 1337

GMDD
3, 1317–1357, 2010

Papavergos, P. and Hedley, A.: Particle deposition behaviour from turbulent flows, Chem. Eng. Res. Des., 62, 275–293, 1984. 1330
Paulson, C.: The mathematical representation of wind speed and temperature profiles in the unstable atmospheric surface layer, J. Appl. Meteorol., 9, 857–861, 1970. 1321
Paw U, K.: The rebound of particles from natural surfaces, J. Colloid Interface Sci., 93, 442–452, 1983. 1325
Paw U, K. and Braaten, D.: Experimental Evidence of the importance of rebound in net deposition of particles, Aerosol Sci. Tech., 17, 278–288, 1992. 1325
Petroff, A., Mailliat, A., Amielh, M., and Anselmet, F.: Aerosol dry deposition on vegetative canopies. Part I: Review of present knowledge, Atmos. Environ., 42, 3625–3653, 2008a. 1319
Petroff, A., Mailliat, A., Amielh, M., and Anselmet, F.: Aerosol dry deposition on vegetative canopies. Part II: A new modeling approach and applications, Atmos. Environ., 42, 3654–3683, 2008b. 1318, 1320, 1323
Petroff, A., Zhang, L., Pryor, S., and Belot, Y.: An extended dry deposition model for aerosols onto broadleaf canopies, J. Aerosol Sci., 40, 218–240, 2009. 1318, 1320, 1330, 1335
Pryor, S. and Barthelmie, R.: Particle dry deposition to water surfaces: Processes and consequences, Mar. Pollut. Bull., 41, 220–231, 2000. 1337
Pryor, S., Larsen, S., Sørensen, L., Barthelmie, R., Grönholm, T., Kulmala, M., Launiainen, S., Rannik, Ü., and Vesala, T.: Particle fluxes over forests: Analyses of flux methods and functional dependencies, J. Geophys. Res., 112, D07205, doi:10.1029/2006JD008066, 2007. 1319
Pryor, S., Gallagher, M., Sievering, H., Larsen, S., Barthelmie, R., Birsan, F., Nemitz, E., Rinne, J., Kulmala, M., Grönholm, T., Taipale, R., and Vesala, T.: A review of measurement and modelling results of particle atmosphere-surface exchange, Tellus B, 60, 42–75, 2008. 1319, 1320
Raupach, M.: Simplified expressions for vegetation roughness length and zero-plane displacement as functions of canopy height and area index, Bound.-Lay. Meteorol., 71, 211–216, 1994. 1329
Raupach, M.: Corrigenda – Simplified expressions for vegetation roughness length and zero-plane displacement as functions of canopy height and area index, Bound.-Lay. Meteorol., 76, 303–304, 1995. 1329
Raupach, M., Antonia, R., and Rajagopalan, S.: Rough-wall turbulent boundary layers, Appl.

GMDD
3, 1317–1357, 2010

Mech. Rev., 44, 1–24, 1991. 1332
Ruijgrok, W., Davidson, C., and Nicholson, K.: Dry deposition of particles. Implications and recommendations for mapping of deposition over Europe, Tellus B, 47, 587–601, 1995. 1319
Schmidt, A. and Klemm, O.: Direct determination of highly size-resolved turbulent particle fluxes with the disjunct eddy covariance method and a 12 - stage electrical low pressure impactor, Atmos. Chem. Phys., 8, 7405–7417, doi:10.5194/acp-8-7405-2008, 2008. 1339
Sehmel, G.: Particle eddy diffusivity and deposition velocities for isothermal flow and smooth surfaces, J. Aerosol Sci., 4, 125–138, 1973. 1334, 1353
Sehmel, G. and Hodgson, W.: A model for predicting dry deposition of particles and gases to environmental surfaces, Battelle, Pacific Northwest Laboratories, Tech. Rep. PNL-SA-6721, 1978. 1318
Sehmel, G. and Sutter, S.: Particle deposition rates on a water surface as a function of particle diameter and air velocity, Journal de Recherches Atmospheriques, 8, 911–920, 1974. 1336, 1356
Slinn, W.: Prediction for particle deposition to vegetative canopies, Atmos. Environ., 16, 1785–1794, 1982. 1318, 1319, 1320, 1325
Smith, S.: Coefficients for sea surface wind Stress, heat Flux, and wind profiles as a function of wind speed and temperature, J. Geophys. Res., 92, 15467–15472, 1988. 1336
Tammet, H., Kimmel, V., and Israelsson, S.: Effect of atmospheric electricity on dry deposition of airborne particles from atmosphere, Atmos. Environ., 35, 3413–3419, 2001. 1326
Textor, C., Schulz, M., Guibert, S., Kinne, S., Balkanski, Y., Bauer, S., Berntsen, T., Berglen, T., Boucher, O., Chin, M., Dentener, F., Diehl, T., Easter, R., Feichter, H., Fillmore, D., Ghan, S., Ginoux, P., Gong, S., Grini, A., Hendricks, J., Horowitz, L., Huang, P., Isaksen, I., Iversen, I., Kloster, S., Koch, D., Kirkevåg, A., Kristjansson, J. E., Krol, M., Lauer, A., Lamarque, J. F., Liu, X., Montanaro, V., Myhre, G., Penner, J., Pitari, G., Reddy, S., Seland, Ø., Stier, P., Takemura, T., and Tie, X.: Analysis and quantification of the diversities of aerosol life cycles within AeroCom, Atmos. Chem. Phys., 6, 1777–1813, doi:10.5194/acp-6-1777-2006, 2006. 1318
Waldman, L. and Schmitt, K.: Thermophoresis and diffusiophoresis of aerosols, in: Aerosol science, edited by: Davies, C. N., Academic Press, London, UK, 137–162, 1966. 1326
Wang, Z., Li, J., Wang, X., Pochanart, P., and Akimoto, H.: Modeling of Regional High Ozone Episode Observed at Two Mountain Sites (Mt. Tai and Huang) in East China, J. Atmos. Chem., 55, 253–272, 2006. 1319

GMDD
3, 1317–1357, 2010

Williams, R.: A model for the dry deposition of particles to natural-water surfaces, Atmos. Environ., 16, 1933–1938, 1982. 1337
Wiman, B. and Agren, G.: Aerosol depletion and deposition in forests-a model analysis, Atmos. Environ., 19, 335–347, 1985. 1320
Wood, N.: A simple method for the calculation of turbulent deposition to smooth and rough surfaces, J. Aerosol Sci., 12, 275–290, 1981. 1330
Wu, Y., Davidson, C., and Russell, A.: Controlled wind-tunnel experiments for particle bounceoff and resuspension, Aerosol Sci. Tech., 17, 245–262, 1992a. 1325
Wu, Y., Davidson, C., and Russell, A.: A stochastic-model for particle deposition and bounceoff, Aerosol Sci. Tech., 17, 231–244, 1992b. 1325
Yoshioka, N., Emi, H., Kanaoka, C., and Yasunami, M.: Efficiency of aerosol trapping by an isolated cylinder: gravity and inertia dominant regions, Kagaku Kògaku, 36, 313–319, 1972. 1325
Young, J. and Leeming, A.: A theory of particle deposition in turbulent pipe flow, J. Fluid Mech., 340, 129–159, 1997. 1334
Zakey, A. S., Solmon, F., and Giorgi, F.: Implementation and testing of a desert dust module in a regional climate model, Atmos. Chem. Phys., 6, 4687–4704, doi:10.5194/acp-6-4687-2006, 2006. 1319
Zhang, K., Knipping, E., Wexler, A., Bhave, P., and Tonnesen, G.: Size distribution of sea-salt emissions as a function of relative humidity, Atmos. Environ., 39, 3373–3379, 2005. 1324
Zhang, L. and Vet, R.: A review of current knowledge concerning size-dependent aerosol removal, China Part., 4, 272–282, 2006. 1320, 1336
Zhang, L., Gong, S., Padro, J., and Barrie, L.: A size-segregated particle dry deposition scheme for an atmospheric aerosol module, Atmos. Environ., 35, 549–560, 2001. 1318, 1319, 1320, 1324, 1325, 1335, 1336, 1337, 1338, 1354, 1355, 1356, 1357
Zhang, L., Brook, J. R., and Vet, R.: A revised parameterization for gaseous dry deposition in air-quality models, Atmos. Chem. Phys., 3, 2067–2082, doi:10.5194/acp-3-2067-2003, 2003. 1318, 1320, 1332
Zufall, M., Davidson, C., Caffrey, P., and Ondov, J.: Airborne concentration and dry deposition fluxes of particulate species to surrogate surfaces deployed in southern Lake Michigan, Environ. Sci. Technol., 32, 1623–1628, 1998. 1336, 1356

GMDD
3, 1317–1357, 2010

Table 1. Parameterization of the deposition efficiencies over vegetation.

Process	Needle-like obstacles	Leaf or plane obstacles
Brownian diffusion	$C_B Sc^{-2/3} Re_h^{-1/2}$	
Interception	$C_{IN} \frac{d_p}{L}$	$C_{IN} \frac{dp}{L} \left[2 + \ln \frac{4L}{d_p}\right]$
Impaction	$C_{IM} \left[\frac{St_h}{St_h + \beta_{IM}}\right]^2$	
Turbulent impaction	$2.5 \times 10^{-3} C_{IT} \tau_{ph}^{+2}$ if $\tau_{ph}^{+} < 20$	
	C_{IT} if $\tau_{ph}^{+} \geq 20$	

GMDD
3, 1317–1357, 2010

Table 2. Coefficients for different Land Use Categories (LUC). The obstacle shape chosen to represent the LUC is given in brackets as N for needle and L for leaf or plane obstacles.

	LUC	h (m)	z_0 (m)	d (m)	LAI 2-sides	L (cm)	C_B	C_{IN}	C_{IM}	β_{IM}	C_{IT}
1	water	–	$f(u)$	0	–	–	–	–	–	–	–
2	ice	–	0.01	0	–	–	–	–	–	–	–
3	inland lake	–	$f(u)$	0	–	–	–	–	–	–	–
4	evergreen needleleaf (N)	15	0.9	12	10	0.15	0.888	0.810	0.162	0.60	0
5	evergreen broadleaf (L)	33.33	2	26.67	12	4	1.262	0.216	0.130	0.47	0.056
6	deciduous needleleaf (N)	15	0.4–0.9	12	0.2–10	0.15	0.888	0.810	0.162	0.60	0
7	deciduous broadleaf (L)	16.67	0.4–1.	13.33	0.2–10	3	1.262	0.216	0.130	0.47	0.056
8	tropical broadleaf (L)	41.67	2.5	33.33	12	4	1.262	0.216	0.130	0.47	0.056
9	drought deciduous forest (L)	16.67	0.6	13.33	8	3	1.262	0.216	0.130	0.47	0.056
10	evergreen broadleaf shrubs (L)	1.54	0.2	0.98	6	2	0.930	0.140	0.086	0.47	0.014
11	deciduous shrubs (L)	1.54	0.05–0.2	0.98	1–6	2	0.930	0.140	0.086	0.47	0.014
12	thorn shrubs (L)	1.54	0.2	0.98	6	2	0.930	0.140	0.086	0.47	0.014
13	short grass and forbs (N/L)	0.31	0.04	0.20	2	0.5	0.700/ 0.996	0.700/ 0.191	0.191/ 0.191	0.60/ 0.47	0.042/ 0.042
14	long grass (L)	0.15–0.77	0.02–0.10	0.10–0.49	1–4	1	0.996	0.162	0.081	0.47	0.056
15	crops (L)	0.15–0.77	0.02–0.10	0.10–0.49	0.2–8	3	0.996	0.162	0.081	0.47	0.056
16	rice (L)	0.15–0.77	0.02–0.10	0.10–0.49	0.2–12	2	0.996	0.162	0.081	0.47	0.056
17	sugar (L)	0.15–0.77	0.02–0.10	0.10–0.49	0.2–10	4	0.996	0.162	0.081	0.47	0.056
18	maize (L)	0.15–0.77	0.02–0.10	0.10–0.49	0.2–8	5	0.996	0.162	0.081	0.47	0.056
19	cotton (L)	0.15–1.54	0.02–0.2	0.10–0.98	0.2–10	7	0.996	0.162	0.081	0.47	0.056
20	irrigated crops (L)	0.38	0.05	0.25	10	3	0.996	0.162	0.081	0.47	0.056
21	urban (N/L)	17	1	11.90	1	0.15/3	0.888/ 1.262	0.810/ 0.216	0.162/ 0.130	0.60/ 0.47	0/ 0.056
22	tundra (N)	0.23	0.03	0.14	0.2–4	0.5	0.700	0.700	0.191	0.60	0.042
23	swamp (L)	0.77	0.1	0.49	8	0.2–4	0.996	0.162	0.081	0.47	0.056
24	desert	–	0.04	–	0	–	–	–	–	–	–
25	mixed wood forest* (N/L)	15	0.6–0.9	12	6–10	0.15/3	0.888/ 1.262	0.810/ 0.216	0.162/ 0.130	0.60/ 0.47	0/ 0.056
26	transitional forest* (N/L)	15	0.6–0.9	12	6–10	0.15/3	0.888/ 1.262	0.810/ 0.216	0.162/ 0.130	0.60/ 0.47	0/ 0.056

* For the mixed wood forest and transitional forest, the deposition velocity for the evergreen needleleaf forest (LUC 4) and for the deciduous broadleaf forest (LUC 7) are calculated and the resulting deposition velocity for the mixed wood forest and the transitional forest is estimated as the average weighted by the proportion of tree types.

GMDD
3, 1317–1357, 2010

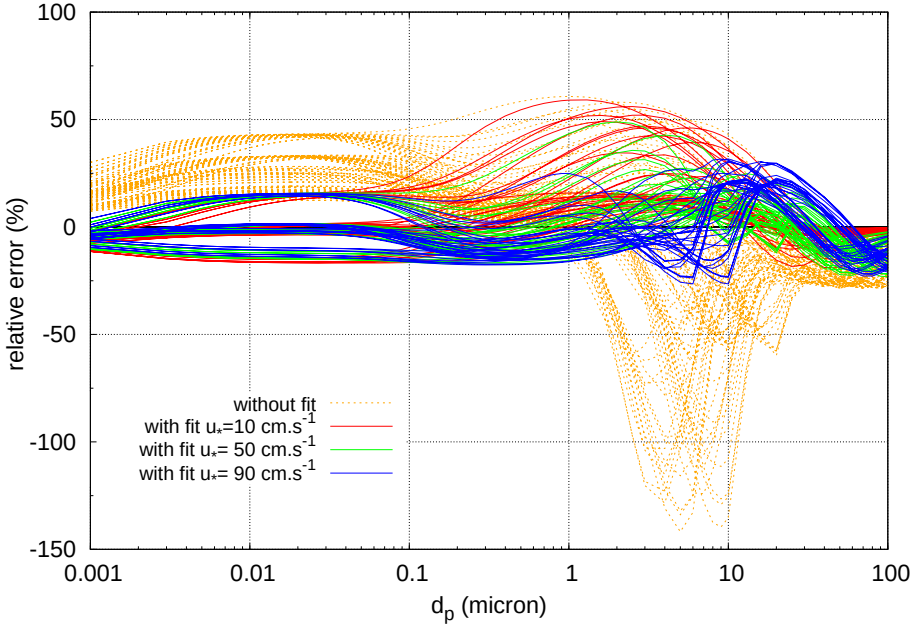

Fig. 1. Comparison on long grass (LUC 14) of the relative errors between the 1-D-model and the present model. Dashed orange lines are results when the present model is not fitted and run on the 96 configurations corresponding to variations of the friction velocity, the obstacle dimension, the ratios z_0/h and d/h, LAI and the particle density. Plain red, green and blue lines are results when the present model is fitted and run on the same 96 configurations (each color corresponds to a friction velocity value).

GMDD
3, 1317–1357, 2010

Analytical model for aerosol dry deposition

A. Petroff and L. Zhang

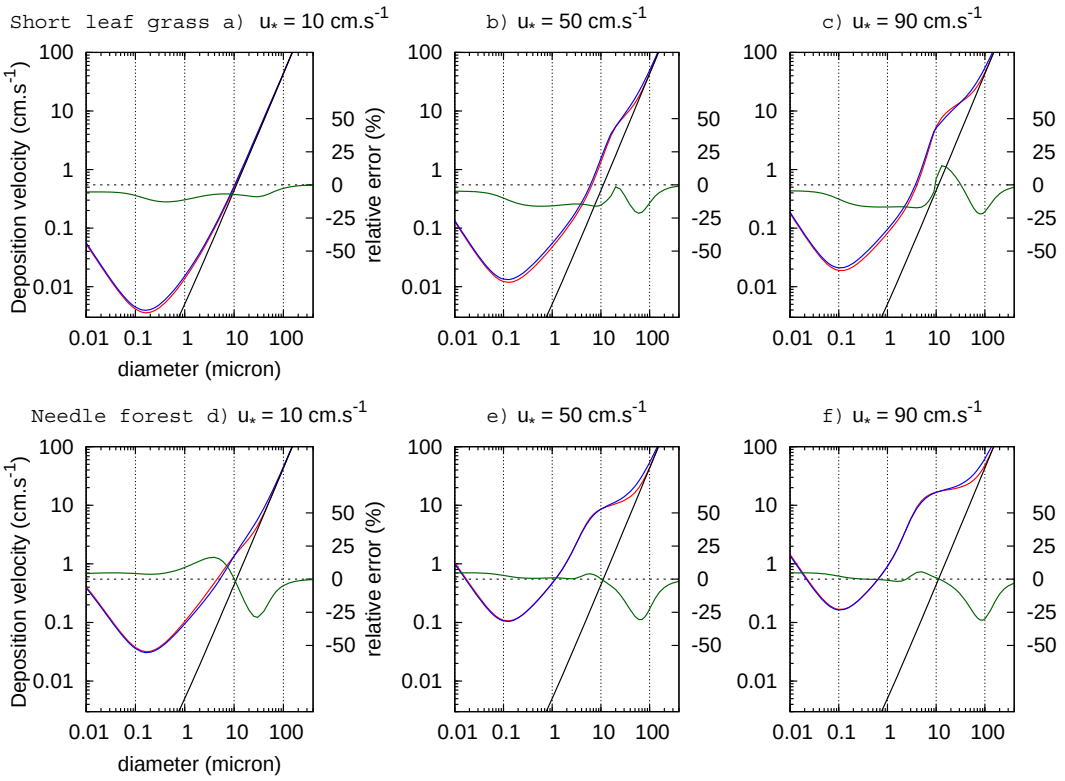

Fig. 2. Comparison of the present model and the 1-D-model under configurations of evergreen needleleaf forest (LUC 4) and short grass (LUC 13, with leaves) for different friction velocity conditions. For the 1-D-model, the crown base height of the forest is taken as $h/2$ and the vertical profile of the leaf surface density as gaussian. Other parameters are given in Table 2. Blue and red plain lines correspond respectively to the present model and the one-dimensional model, while the green plain line corresponds to the relative error between them. The black line corresponds to the sedimentation velocity.

GMDD
3, 1317–1357, 2010

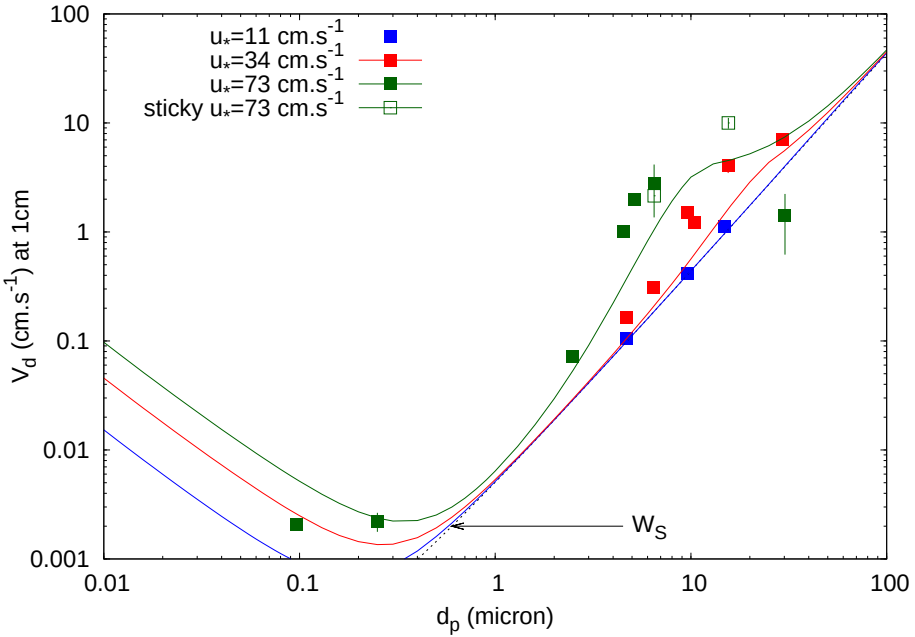

Fig. 3. Deposition on smooth soil, as measured – mean, standard deviation – by Sehmel (1973) and predicted by the present model (plain lines) for friction velocities of 11 cm s^{-1} (blue), 34 cm s^{-1} (red), 74 cm s^{-1} (green).

GMDD
3, 1317–1357, 2010

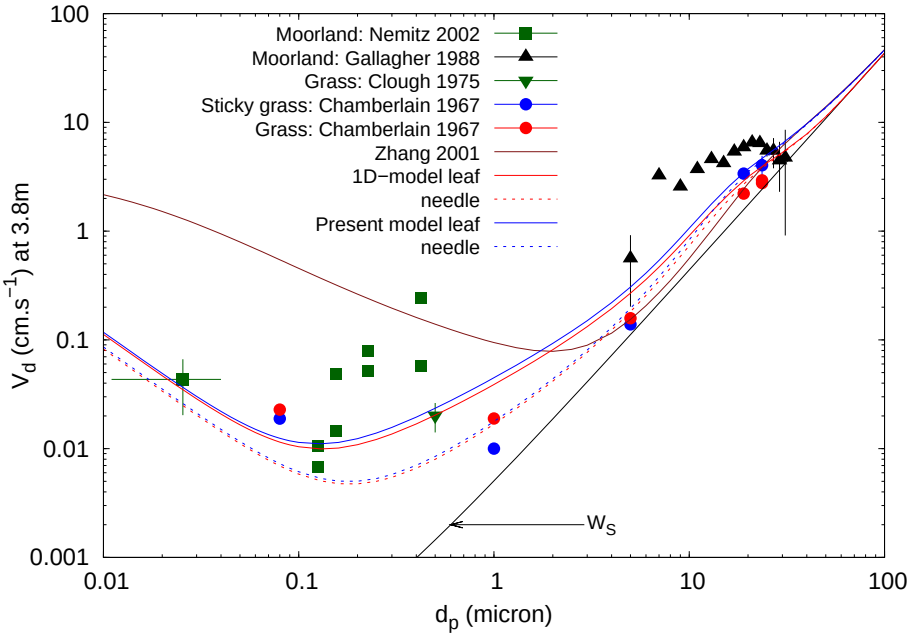

Fig. 4. Deposition on grass, as measured by Chamberlain (1967); Clough (1975); Garland (1983); Gallagher et al. (1988); Nemitz et al. (2002) for friction velocity between 25 and 55 cm s^{-1}. A friction velocity of 40 cm s^{-1} is used to run the model of Zhang et al. (2001, in brown), the 1-D-model on leaf and needle obstacles (red plain and dash) and the present model on leaf and needle obstacles (blue plain and dash). All deposition velocities are re-calculated at z_R=3.8 m. The particle density is taken as ρ_p=1500 kg m^{-3}.

GMDD
3, 1317–1357, 2010

Analytical model for aerosol dry deposition

A. Petroff and L. Zhang

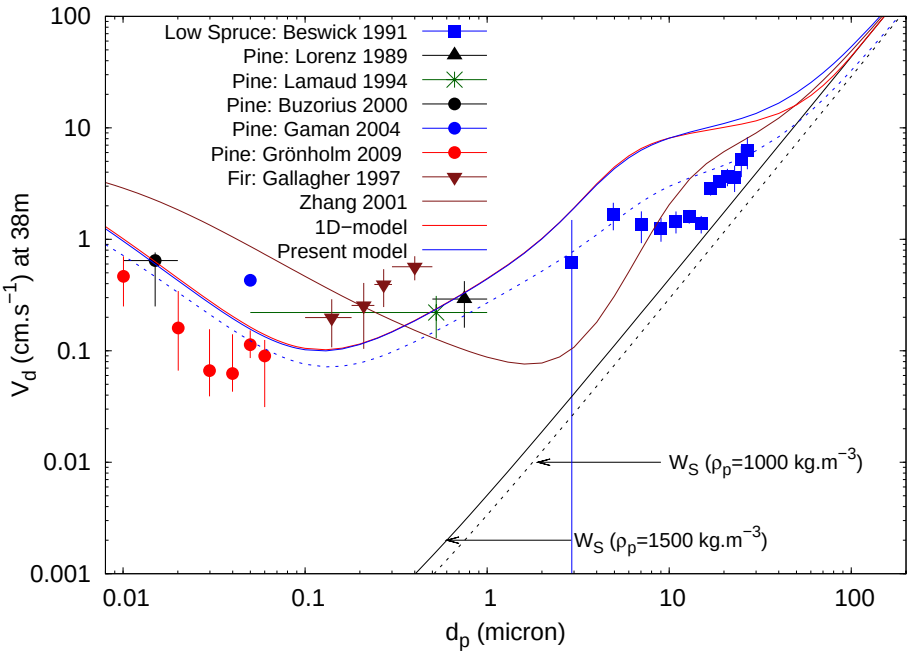

Fig. 5. Deposition on coniferous forest, as measured by Beswick et al. (1991); Lorenz and Murphy (1989); Lamaud et al. (1994); Buzorius et al. (2000); Gaman et al. (2004); Grönholm et al. (2009); Gallagher et al. (1997). A friction velocity of 47.5 cm s^{-1}, a particle density of 1500 kg m^{-3} and the parameters of the LUC 4 are used to run the model of Zhang et al. (2001, in plain brown), the 1-D-model (in plain red) and the present model (in plain blue). Are added in blue dots the predictions of the present model obtained under the configuration of Beswick et al.'s spruce: h=4.2 m, h_c=1 m, LAI=10, z_0=0.3 m and d=2.8 m, ρ_p=1000 kg m^{-3}. All deposition velocities are re-calculated at z_R=38 m.

GMDD
3, 1317–1357, 2010

Analytical model for aerosol dry deposition

A. Petroff and L. Zhang

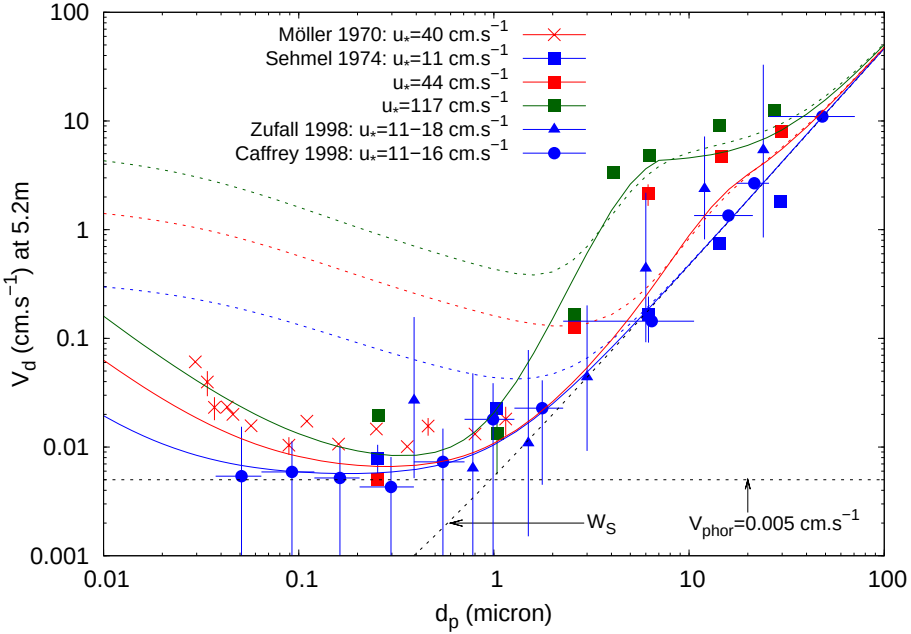

Fig. 6. Deposition on water surfaces, as measured by Möller and Schumann (1970); Sehmel and Sutter (1974); Zufall et al. (1998); Caffrey et al. (1998). The present model (plain) and the model of Zhang et al. (2001, dash) are run for $u_* = 11\,\mathrm{cm\,s^{-1}}$ (blue), u_*=44 $\mathrm{cm\,s^{-1}}$ (red) and u_*=117 $\mathrm{cm\,s^{-1}}$ (green). All deposition velocities are re-calculated at z_R=5.2 m. The particle density is taken as ρ_p=1600 $\mathrm{kg\,m^{-3}}$.

GMDD
3, 1317–1357, 2010

Analytical model for aerosol dry deposition

A. Petroff and L. Zhang

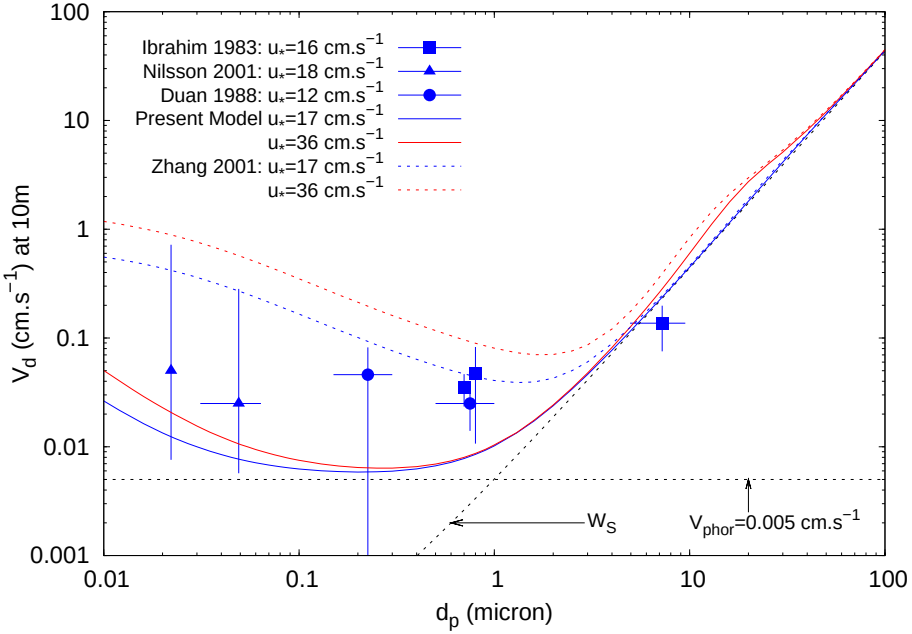

Fig. 7. Deposition on snow surfaces, as measured by Ibrahim et al. (1983); Duan et al. (1988); Nilsson and Rannik (2001). The present model (plain) and the model of Zhang et al. (2001, dash) are run for u_*=17 cm s^{-1} (blue) and u_*=36 cm s^{-1} (red) for an air temperature of 273 °K (0 °C) and $z_0 = 10^{-3}$ m. All deposition velocities are re-calculated at z_R=10 m. The particle density is taken as ρ_p=1500 kg m^{-3}.

GMDD
3, 1317–1357, 2010

Analytical model for aerosol dry deposition

A. Petroff and L. Zhang